

Calculating SAR in Two Models of the Human Head Exposed to Mobile Phones Radiations at 900 and 1800 MHz

S. Khalatbari¹, D. Sardari¹, A. A. Mirzaee¹, and H. A. Sadafi²

¹Amirkabir University, Iran

²Royal Melbourne Hospital, Australia

Abstract—Since the 1990's, use of mobile phones has augmented worldwide generating a public concern as to whether frequent utilization of such devices is unsafe. This provoked EMF researchers to find suitable techniques of assessing radiation blueprint and exposure hazards if any. Most research groups focused on two techniques: experimental measurements and finite-difference time-domain (FDTD) computations. Computation of the specific absorption rate (SAR) generated by cellular phones inside two models of the human head is presented in this paper. Two models of mobile phones were considered working at 900 and 1800 MHz bands according to the Global System for Mobile Communication. Radiated energy distributions and averaged SAR values in 1g and 10g of tissue were computed inside the models of head using FDTD. Computations were compared with a realistic head model constructed with the MRI scans. The distribution of the local SAR in the head was similar to that of the simplified head models. The maximum local SAR calculated was 53.43 W/kg and the maximum SAR(10g) was 2.96 W/kg, both for 1 W output power from the antenna. The results indicated the area of the maximum local SAR was situated in outer layer of skull, where muscle and skin were. The important parameters in absorbed energy in the head were the type of antenna, current distribution and the distance between head and antenna. The head models used for simulation proved as insignificant parameter in the calculations.

1. Introduction

Within only the last ten years, mobile phone usage has been rapidly spread globally. In chorus with the expanding usage, a question has been raised repeatedly as to whether frequent usage of such a device which radiates GHz electromagnetic field onto the human head is unsafe. This rapid expansion has thus pushed the research toward the necessity of finding a reliable means of analyzing mobile phone for radiation pattern performance to address the safety concerns. It is broadly accepted that mobile phones cause heating of the human organ exposed to their radiation and specifically the human head. The current exposure limits are based on Specific Absorption Rate (SAR) of the exposure heat. A SAR limit of 2 W/kg averaged over any contiguous 10g head tissue was recommended by the Council of European Union [1] for the general public. This recommendation in a way acknowledged that a simple cubical geometry used may yield calculated dosimetric quantities of conservative values corresponding to the exposure guidelines.

It has been a while since, most research groups studying biological effects of mobile phones have focused on two methods: *experimental measurements* and *finite-difference time-domain* (FDTD) computations [2-5]. While experimental measurements make use of the actual mobile phone being tested [6], there remains a question of appropriateness of representing the human head with simplified phantoms that for compliance testing include, at most, two or three tissue type materials [4, 5]. The FDTD method, on the other hand, can be questioned on its lack of a realistic anatomically heterogeneity representation of the radiation exposure of mobile phone through the human head model [7].

In the research work reported here, the authors focused on the absorption of energy in the human head from near-field radiation of wireless phones. Two models for mobile phone (half-wavelength dipole and a quarter-wavelength monopole) and two simple models for head (homogenous and multi-layer spherical) were considered. A modern method for calculating maximum SAR (10g) was introduced and the results were compared with a realistic MRI model of head [6, 7].

2. Numerical Method and Modeling

Two models used for the human head were spheres of 20 cm diameter. The first model was a sphere consisting entirely of material with the electric properties of brain tissue. The second model comprised three layers as illustrated in Fig. 1. The spherical model had a uniform content at its core (representing the human brain) and the core was surrounded by two spherical shells representing the skull (bone) and the muscle and skin (skin) with their respective electromagnetic properties.

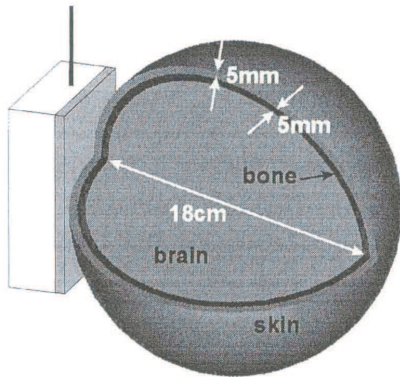


Figure 1: The model of the layered sphere.

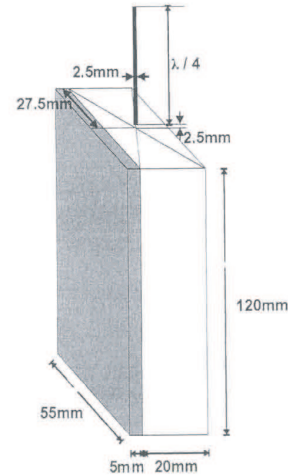


Figure 2: The model of the monopole antenna mounted on top of the metal box.

The handset has been modeled in two different ways, namely a half-wavelength dipole and a quarter-wavelength monopole both mounted on top of a metal box. The thickness of the antennas in both cases was one FDTD cell. The antennas were centered on the top surface of a conducting box with dimensions 120 mm × 55 mm × 20 mm (see Fig. 2). The face of the metal box next to the user was covered with a dielectric material of 5 mm thickness. The feeding gap of the dipole antenna was placed at a distance of 0.5 mm from the sphere. However, the feeding gap of the monopole antenna located 2 cm away from the sphere, since the minimum distance between the sphere and metal box was again 0.5 cm [4, 5, 8].

The simulation was performed at the two common telecommunication carrier frequencies of 900 MHz and 1800 MHz. The handset antenna model length was adjusted according to the wavelength in free space obviously corresponding to the frequency in use. Combinations of the cases were also investigated as detailed in Table 1. The properties of tissue material considered in the computer simulation modeling at both frequencies [3] were as tabulated in Table 2.

Table 1: Description of the cases examined.

Case	Homogeneous Sphere	Layered Sphere	900 MHz	1800 MHz	Dipole	Monopole
1	*		*		*	
2	*		*			*
3	*			*	*	
4	*			*		*
5		*	*		*	
6		*	*			*
7		*		*	*	
8		*		*		*

A software sourced from the Utah University of Technology (<http://www.fDTD.org>) was used for the simulation. The lattice for all cases was formed by a uniform rectilinear grid with a space step of 2.5 mm in all three directions. The simulation time was twenty periods of the source signal. A hard source model was positioned at the feeding gap, which had the size of one cell [3, 9–12]. The source had a sinusoidal time behavior and was switched on at the beginning of the computer run. In all simulations the output power of the antenna was 1 W. Mur's second-order absorption boundary conditions [13, 14] were used to truncate the computational domain.

The distribution of the local SAR values can be calculated directly from the electric field distribution, which results from the computer run. This was achieved using Eq. (1) as the sinusoidal source leads to a steady state electric field, numerically analogous with the same sinusoidal variation [3–6].

$$SAR = \frac{\sigma E_{\max}^2}{2\rho} \quad (1)$$

Table 2: The properties of the materials used in the simulations.

Material	900 MHz ϵ_r	900 MHz σ	1800 MHz ϵ_r	1800 MHz σ	Mass Density (Kg/m ³)
<i>Skin</i>	39.5	0.7	38.2	0.9	1080
Bone (cortical)	12.5	0.17	12.0	0.29	1180
Brain (Grey matter)	56.8	1.1	51.8	1.5	1050
Dielectric Phone Cover	2.7	0.0016	2.7	0.003	-

To test the hypothesis that steady state was reached after twenty periods of the numerical source signal, the time evolution of the electric field at several points in the lattice was monitored during each computer run [3, 7, 15]. It was found that for all the cases examined, the simulation time was more than enough to arrive at steady state.

The derivation of the average SAR values needs some post-processing of the simulation results. The SAR values were averaged over 1 g and 10 g of tissue. The way averaging volume was selected was crucial for the derived average SAR distributions [3, 7, 15]; hence the averaging procedure adopted had to be clarified. The edge of each cell in the lattice was 2.5 mm which allowed for a 1 cm cube to be considered per four cells. This cube provided 1 g of tissue for a mass density of 1 g/cm³. Noting that the area of SAR (10 g) was situated outside of the skull area (in the muscle) and the size of the cube was sufficiently small. Therefore, the computation output results allowed direct calculation of the maximum SAR. Conversely, it was impossible to have a cubic volume of tissue with a mass of 10 g; and, as in the previous method a cube of 2.25 cm sides (nine cells) was considered (method 1). In this case, due to the long length of the cube and its location with different SAR specially in between skull/brain and skull/muscle, the calculations resulted in a noticeable difference with previously published studies. The process details were reviewed and checked again and found to be precise. Furthermore, two cubes were considered, 1.75 cm³ (seven cells) and 2.25 cm³ (nine cells) co-centered as illustrated in Fig. 3. The SAR (10 g) value was subsequently calculated considering the contribution of the smaller cube and the contribution of the cubical shell around it each with a predefined weighting coefficient using Eq. (2).

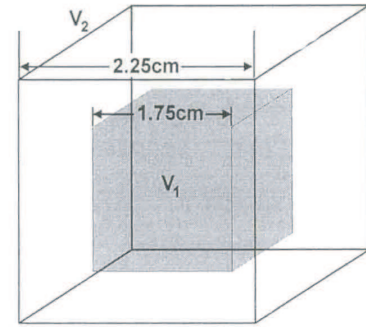


Figure 3: The cube volumes used for calculating the SAR (10 g) values.

$$SAR(10g) = \frac{\sum_{v_1} (SAR)_i m_i + \sum_{v_2-v_1} (SAR)_j m_j}{\sum_{v_1} m_i + \sum_{v_2-v_1} m_j} \quad (2)$$

where $m_i = \rho_i \Delta V$ and $m_j = \rho_j \Delta V \frac{10-V_1}{V_2-V_1}$ [3]. Index i refers to the lattice cells inside the inner cube and index j to those around it (method 2).

Table 3: Total absorbed power, maximum SAR(1g), maximum SAR(10g) and local SAR in the head model (antenna output power 1 W).

Case	P_{abs} (W)	$SAR(1g)_{max}$ (W/kg)	$SAR(10g)_{max}$ (W/kg) (Method 1)	$SAR(10g)_{max}$ (W/kg) (Method 2)	Local SAR_{max} (W/kg)
1	0.77	2.45	2.96	1.89	26.19
2	0.41	0.74	0.82	0.53	4.23
3	0.75	4.67	6.15	3.89	70.16
4	0.24	0.52	0.63	0.41	3.92
5	0.76	1.64	1.91	1.22	18.86
6	0.48	0.5	0.58	0.37	3.72
7	0.83	4.13	5.01	3.18	54.14
8	0.30	0.59	0.69	0.44	4.87

3. Results

Table 3 presents a summary of the total absorbed power, the maximum SAR (1 g), the SAR (10 g) and local SAR values. These results indicated that the model of the handset device played a more important role in dosimetry than the model of human head. This was evident when looked at the difference in calculated values; for instance, considering case 1 (homogeneous sphere, 900 MHz, $\lambda/2$ dipole) with case 5 (layered sphere, 900 MHz, $\lambda/2$ dipole) yielded smaller figures than when the case 1 was considered with case 2 (layered sphere, 900 MHz, $\lambda/4$ monopole). As reported previously [4, 5, 8], this research confirmed that in most cases the homogeneous sphere resulted in a larger SAR values than the layered sphere. It was also apparent from the results in Table 3 that modeling the handset as a dipole yielded higher SAR values than modeling it as a monopole.

However a direct comparison between the respective pairs of cases was not possible, because it could be argued that the smaller distance of the dipole feeding gap to the head may account for the larger SAR values. So, the distance of the $\lambda/2$ dipole was varied for case 3 (homogeneous sphere, 1800 MHz, $\lambda/2$ dipole) to study its significance. As shown in Fig. 4, at 2 cm distance the values obtained with the $\lambda/2$ dipole are still larger than case 4 (homogeneous sphere, 1800 MHz, $\lambda/4$ monopole). It can be noted from Fig. 4 that the maximum local SAR doesn't fall off inversely proportional to the square of distance, as it would in the far field.

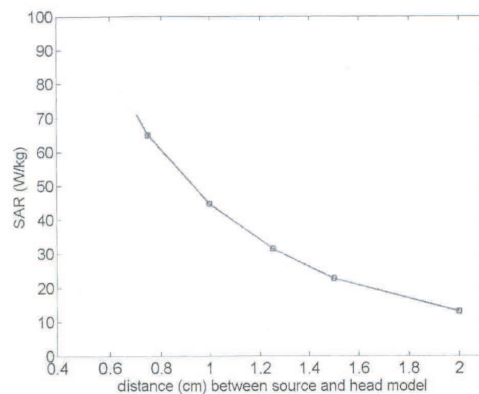


Figure 4: Variation of maximum local SAR values.

The effect of different operating frequencies was as illustrated in Fig. 5 and Fig. 6. An observation was that the SAR decreased faster in the higher frequency range as expected due to the smaller penetration depth.

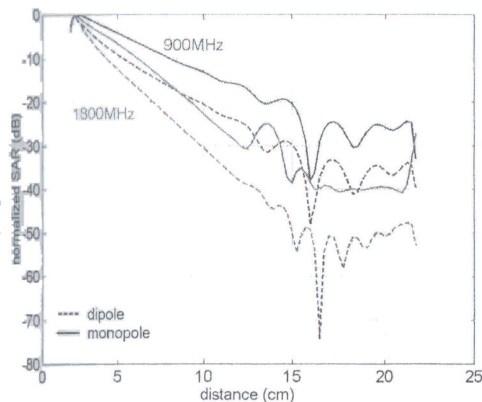


Figure 5: The profile of local SAR across the homogeneous spherical head model. The distance was measured from the point of the source closest to the head model. The SAR values were normalized to the maximum to show the effect of frequency.

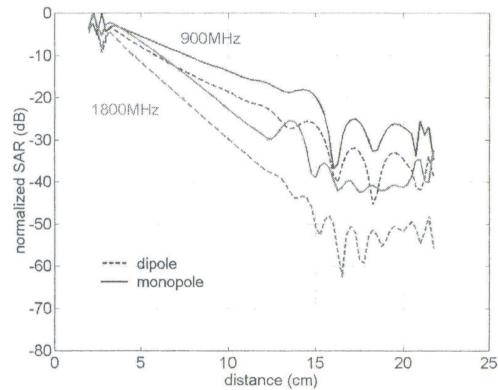


Figure 6: The profile of local SAR across the layered spherical head model. The distance was measured from the point of the source closest to the head model. The SAR values were normalized to the maximum to show the effect of frequency.

4. Comparison between Case Study and MRI Human Head Model

The MRI model used in this work was the Bradford University Telecommunication Research Center Tissue-classified high-resolution voxel image of a human head [6, 7]. The original resolution of the model was 0.909 mm

in the x and y direction on the axial plane and 1.480 mm in the z (vertical) direction. The phantom was re-sampled to have cubic voxels with each side of 0.25 mm length. A $\lambda/4$ monopole on top of a metal box was used for the device model, with the source operating at 900 MHz. The distribution of the local SAR in the head (Fig. 7) was similar to that of the simplified head models. The maximum local SAR calculated was 53.43 W/kg and the maximum SAR(10 g) was 2.96 W/kg, both for 1 W output power from the antenna.

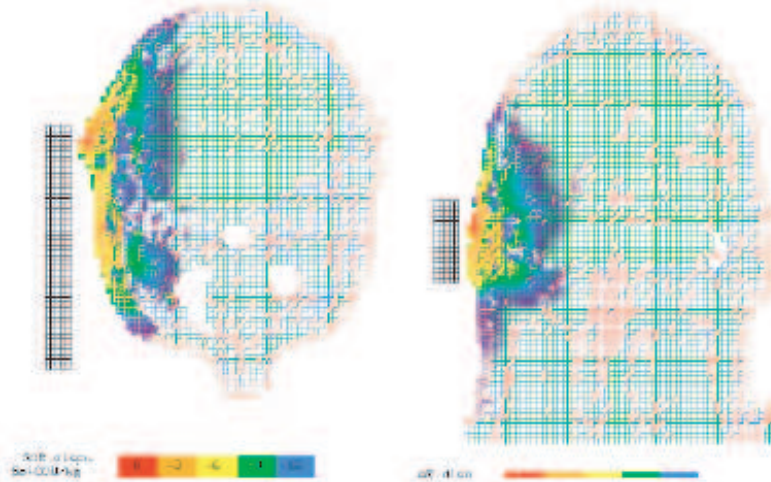


Figure 7: Distribution of the local SAR on a) the middle coronal plane and b) the middle axial plane of the MRI head model for the monopole on top of the Box operating at 900 MHz. The values are normalized to the maximum local SAR.

5. Discussion and Conclusions

The maximum SAR(10 g) value was higher than the basic limit of 2 W/kg SAR(10 g) over 6 minute period according to the widely adopted exposure guidelines [1]; however, the following points must be noted:

1)In the simulations, it was assumed that the device was operating continuously. Nevertheless, time-averaged power of a GSM device under real operating conditions was 1/8 of its nominal power. Therefore, for a nominal operating power of 1W the actual time-averaged output power was 0.125W [see also 3-5, 7, 8, 15].

2)The introduction of a dielectric scatterer like the human head in the vicinity of the radiating antenna alters the input impedance of the latter. In the calculations it was assumed that all the power generated and transmitted by the electronic devices to the antenna was fully radiated out; i.e., the antenna and the transmission line were completely matched. This assumption represented the worse case since only a portion of the power was radiated from the antenna.

3)It was shown that the use of a metal box model for the phone instead of a CAD model gives more conservative results, i.e., higher SAR values [6].

Although the total absorbed power in most cases was lower for 1800 MHz than for 900 MHz, the maximum SAR values are higher for the higher frequency. The distribution of SAR in the spherical head models shown as in Fig. 7, indicated that the large SAR values were restricted within a volume close to the surface of the model. In fact, in more than 94% of the head model volume the SAR was smaller than 10% of the local maximum SAR for each case (see Fig. 8).

Finally, the results demonstrated that the area of the maximum local SAR was situated in outer layer of skull, where muscle and skin were located. Since the maximum difference in dielectric properties between muscle and skull was more than other tissues, the maximum reflection happened around the boundary of the

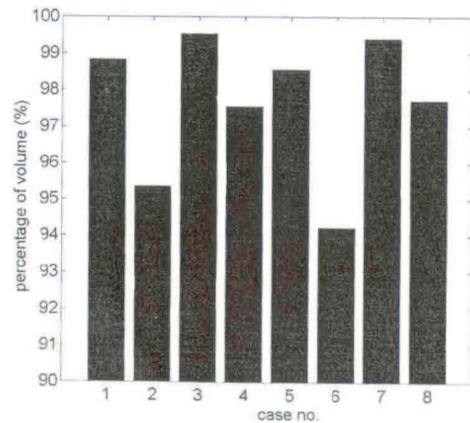


Figure 8: Percentage of volume in the spherical head models for which the local SAR has a value smaller than 10% of the maximum local SAR.

two tissues. Thus maximum absorption power was seen in this border; and, because of the skin effect, with increasing frequency the situation of the maximum local SAR would get closer to the outer layer of the head. Also the results showed that the maximum SAR (10 g) was about 20% to 30% lower than maximum SAR (1 g) under similar conditions.

In conclusion, the important parameters affecting the absorbed energy in the human head exposed to mobile phone radiation were the type of antenna, current distribution and the distance between head and antenna; and, head models used for simulation did not play any significant role in the calculations.

REFERENCES

1. "IEEE standard for safety level with respect to human exposure to radio frequency field, 3 KHz to 300 KHz," *Tech. Rep. IEEE C95.1*, 1999.
2. Balzano, Q. and T. J. Manning, "Electromagnetic energy exposure of simulated users of portable cellular telephones," *IEEE Trans.*, Vol. 44, 390–403, Aug. 1995.
3. Stavroulakis, P., *Biological Effects of Electromagnetic Fields*, Springer, 2002.
4. Hombach, V., K. Meier, M. Burkhardt, E. Kastle, and N. Kuster, "The dependence of electromagnetic energy absorption upon human head modeling at 900 MHz," *IEEE Trans. Microwave Theory Tech.*, Vol. 44, 1865–1873, Oct. 1996.
5. Hombach, V., K. Meier, M. Burkhardt, E. Kastle, and N. Kuster, "The dependence of electromagnetic energy absorption upon human head modeling at 1800 MHz," *IEEE Trans. Microwave Theory Tech.*, Vol. 45, 2058–2062, Nov. 1997.
6. Tinniswood, A. D. and O. P. Gandhi, "Computations of SAR distributions for two anatomically based models of the human head using CAD files of commercial telephones and the parallelized FDTD code," *IEEE Trans. Ant.*, Vol. 46, 829–833, 1998.
7. Dimbylow, P. J. and S. M. Mann, "SAR calculations in a anatomically realistic model of the head for mobile communication transceivers at 900 MHz and 1.8 GHz," *Physic in Medicine and Biology*, Vol. 39, 1537–1553, 1994.
8. Watanabe, S., M. Taki, T. Nojimi, and O. Fujiware, "Characteristics of the SAR distributions in a head exposed to electromagnetic fields radiated by a handheld portable radio," *IEEE Trans. Microwave*, Vol. 44, 1874–1883, 1996.
9. Taflove, A., *Advances in Computational Electromagnetics: The Finite Difference Time Domain Method*, Artech House, 1998.
10. Kunz, K. S. and R. J. Luebbers, *The Finite Difference Time Domain Method for Electromagnetics*, CRC Press, 1993.
11. Balanis, C. A., *Advanced Engineering Electromagnetics*, John Willy and Sons, New York, 1989.
12. Volakis, J., A. Chatterjee, and L. C. Kempel, *Finite Element Method for Electromagnetics*, IEEE Press, 1998.
13. Enguist, B. and A. Majda, "Absorbing boundary conditions for the numerical simulation of waves," *IEEE Trans. Electromagnetic*, Vol. 23, 377–382, Nov. 1987.
14. Chew, W. and J. Lin, "Perfectly matched layers in the discretized space," *IEEE Trans. Electromagnetics*, Vol. 16, 325–340, 1996.
15. Gandhi, O. P., G. Lazzi, and C. M. Furse, "Electromagnetic absorption in the human head and neck for mobile telephones at 835 and 1900 MHz," *IEEE Trans. Microwave*, Vol. 44, 1884–1897, 1996.